

Influence of the Macroring Size on the Self-Association Thermodynamics of Cyclodextrins with a Double-Linked Naphthalene at the Secondary Face

M. José González-Álvarez,[†] Juan M. Benito,[‡] José M. García Fernández,[‡] C. Ortiz Mellet,[§] and Francisco Mendicuti*,[†]

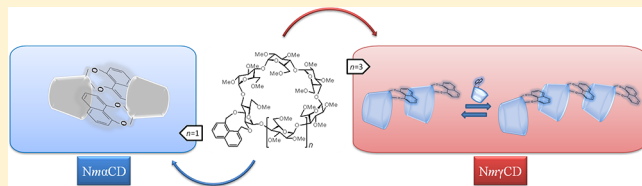
[†]Departamento de Química Física, Universidad de Alcalá, 28871 Alcalá de Henares Madrid, Spain

[‡]Instituto de Investigaciones Químicas (IIQ), CSIC - Universidad de Sevilla, 41092 Sevilla, Spain

[§]Departamento de Química Orgánica, Facultad de Química, Universidad de Sevilla, 41071 Sevilla, Spain

Supporting Information

ABSTRACT: The conformational properties and aggregation behavior of two selectively modified cyclomaltooligosaccharides (cyclodextrins, CDs) containing a double-linked 1,8-dimethylnaphthalene cap-like moiety at the secondary face, namely, 2¹,3¹-O-(1,8-dimethylnaphthalene- α,α' -diyl)-per-O-Me- α - and γ -cyclodextrins (Nm α CD and Nm γ CD, respectively), in water and in organic solvents were investigated. Both CD derivatives self-associated in water to form dimer species, but the characteristics of the dimerization process and of the resulting dimer strongly depended on the size of the macrocycle. Dimerization constants, thermodynamic parameters upon association, and information about the preferred conformations of the monomer and dimer CD structures were obtained by using NMR, UV-vis, steady-state and time-resolved fluorescence, and circular dichroism experimental techniques, as well as molecular mechanics (MM) and molecular dynamics (MD) simulations. The complexation of 1,8-di(methoxymethyl)naphthalene (oNy) and the heteroassociation of both NmCDs with their permethylated CD partners (*m*CDs), lacking the aromatic cap, were examined. In addition, the influence of the size of the chromophore moiety on the thermodynamics of self-association was also assessed by comparison of the results obtained for the new naphthalene derivatives with those of the 2¹,3¹-O-(1,2-xylylene)-modified CD analogues (XmCDs).



INTRODUCTION

Cyclodextrins (CDs) are natural cyclic oligosaccharides formed of $\alpha(1\rightarrow 4)$ -linked D-glucopyranose units. The three most common CDs are the hexamer (α -cyclodextrin), heptamer (β -cyclodextrin), and octamer (γ -cyclodextrin). All of them are water-soluble, natural products featuring a basket-shaped architecture with two well differentiated faces bearing the primary (narrower) and secondary hydroxyls (wider), respectively, and a hydrophobic cavity that can include guest molecules of appropriate size, thereby acting as molecular containers.^{1,2} Chemical modifications of the natural cyclodextrins have attracted widespread interest in order to increase their water solubility, improve their binding properties, and enhance their chiral selectivity, molecular recognition, and molecular self-assembling abilities.^{3–6} In this context, CD conjugates bearing a chromophore substituent^{7–9} are especially interesting due to their potential as chemo-sensors,^{7,10} photochemical microreactors,^{8,9} and antenna host molecules.^{11–14} Within fluorescent CDs, naphthalene-modified cyclodextrins have been extensively investigated as light harvesting host molecules,^{11,15} building blocks for functional supramolecular architectures,^{16,17} catalysts,¹⁸ and in sensing applications.^{19–21}

Fluorescently labeled CD derivatives and their complexes are also useful tools for real-time monitoring of events involving their interaction with biological receptors or biomacromolecules.^{22–24} Controlling the self-association properties through face-selective modification is a general prerequisite for those channels.²⁵ Thus, the installation of hydrophobic moieties at the secondary face of CDs facilitates the formation of head-to-head bilayers upon interaction with nucleic acids, which is critical to generate transfectious nanocomplexes.^{26–29} Notably, the size of the cyclooligosaccharide ring has been shown to have a strong impact in this process.³⁰ In this context, the possibility to use naphthalene moieties to simultaneously endow the system with fluorescent and self-assembling properties seemed very appealing.

The majority of the reports about naphthalene functionalized CDs focus on β CD architectures. Derivatives of α - and γ -modified CDs are very rarely described, despite the distinct inclusion properties of their cavities.^{31,32} Thus, the smallest α CD cavity size is appropriate for forming favorable inclusion complexes with a wide variety of small molecules³¹ and linear

Received: January 23, 2013

Revised: April 1, 2013

Published: April 16, 2013

polymers (pseudopolyrotaxanes).^{33,34} The biggest γ CD homologue can be used as a molecular flask in which two guest molecules can meet and react in the cavity, and the formation of charge transfer complexes and excimers has actually been shown to be promoted inside the γ CD cavity.^{35–40}

Ueno and co-workers^{41–47} have pioneered research on modified CDs bearing naphthyl substituents at the primary face. In one of their first works, they compared the conformational behavior of modified γ CDs bearing one or two single-linked naphthalene groups at the primary side in the presence of different guest molecules.^{41,42,48} If only a single aromatic moiety is appended to the γ CD, and it is capable of self-inclusion into the cavity, it acts by narrowing the large γ CD cavity and then favoring the formation of 1:1 stoichiometry complexes with the guest. The complexation behavior may be regarded as an induced-fit type of complexation, since the appended group changes its location so as to be suited for guest binding.^{41,47} When two naphthyl moieties are present, the results indicated that both are simultaneously located inside the γ CD cavity. In the presence of guest molecules, the two chromophores come out of the cavity, remaining close to each other and acting as hydrophobic caps.^{42,48} Depending on the guest and relative location of the naphthyl substituents in the γ CD primary rim, diverse circular dichroism and fluorescence responses were exhibited,⁴⁹ which was useful for sensing and detection of several organic guest molecules.^{50–52}

In contrast to that observed for naphthyl- γ CD conjugates, β CD derivatives containing a single naphthyl moiety at the primary face formed dimers.⁴⁴ Derivatives bearing two naphthyl groups exhibited a conformational equilibrium between two forms, one having a single naphthalene group included in the cavity and another in which both naphthalenes were placed outside the cavity acting as a cap. The latter conformation was more abundant at high concentrations of the guest.⁵³ The same authors reported supramolecular light-harvesting antenna polyrotaxanes by using canonical α CDs and naphthalene appended α CDs, in different ratios, threaded on a poly(ethylene glycol) (PEG) chain with anthracene,⁵⁴ dansyl,⁵⁵ adamantane,⁵⁶ or trinitrophenyl⁵⁷ units at both ends. The energy migration and/or energy transfer efficiencies from naphthalene to end-groups were examined and related to the CD polyrotaxane composition.

Whereas considerable efforts have been devoted to investigate the complexation of naphthalene modified CDs with different guests,^{18–21,58,59} just a few reports concern the possible self-association processes in water solution. The group of J. W. Park has reported the synthesis of modified cyclodextrins with various chromophores at the primary side,^{60–64} including 6-O-(2-sulfonate-6-naphthyl)- β ⁶¹ and γ -CD.⁶² These compounds formed noncovalent head-to-head (HH) dimers with quite different dimerization constants (9700 ± 2500 and $140 \pm 50 \text{ M}^{-1}$ at 25°C for the modified β - and γ CD, respectively). To the best of our knowledge, no data are available for naphthalene α CD derivatives and reports on CD derivatives with pendant groups attached at the secondary face are very scarce.^{15,65,66}

Our group reported the synthesis of 2¹,3¹-O-(1,8-dimethyl-naphthalene- α,α' -diyl)-per-O-Me- β -CD ($Nm\beta$ CD).⁶⁶ Thermodynamic studies pointed to the formation of a highly stable dimer in aqueous solution ($K_D \approx 9 \times 10^4 \text{ M}^{-1}$ at 25°C), which dissociated in nonpolar solvents. The dimerization process was both enthalpy and entropy favored. Computational calculations agreed with the experimental evidence, suggesting that head-to-

head oriented dimers are the most stable species in water solution. In these dimer structures, the naphthalene moieties are relatively shielded from the solvent and sufficiently close to each other to couple their transition moments as inferred by the circular dichroism spectra but without forming intermolecular excimers.

In order to predict the behavior of double-like, secondary face naphthalene-capped CDs and their potential to promote ordered structures, a comparative study of their conformational and thermodynamic properties in solution as a function of the CD size was required. Evaluating, understanding, and rationalizing the influence of the appended group and importance of the size of the macrocycle on the dimer stability and conformational behavior were the aim of this work. Studies in that direction could be particularly useful for designing modified cyclodextrins with characteristics that are better suited for promoting interactions with drugs and genetic material.⁶⁷ In this paper, several spectroscopic methods including NMR, UV-vis, steady-state and time-resolved fluorescence, and circular dichroism, as well as molecular modeling techniques, were employed to investigate the conformational and aggregation properties of 2¹,3¹-O-(1,8-dimethyl-naphthalene- α,α' -diyl)-per-O-Me- α - and γ -CD ($Nm\alpha$ CD and $Nm\gamma$ CD, respectively (Figure 1)) in dilute

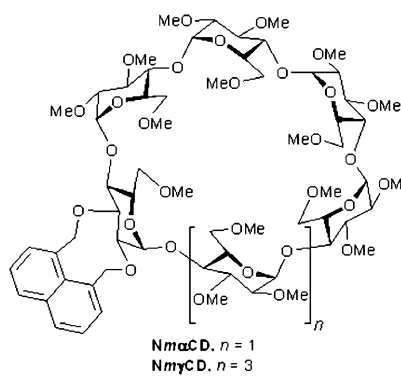


Figure 1. Structure of 2¹,3¹-O-(1,8-dimethyl-naphthalene- α,α' -diyl)-per-O-methyl- α -cyclodextrin (Nm α CD) and γ -cyclodextrin (Nm γ CD).

water solutions and in organic solvents. The dimerization equilibrium constants (K_D) at several temperatures and the thermodynamic parameters associated with these processes have been obtained from the analysis of decay profiles of the naphthalene moiety emission. The contribution of the chromophore group to the self-assembling process was assessed by examining the tendency to form heterodimers with the permethylated analogues lacking the aromatic moiety ($m\alpha$ CD and $m\gamma$ CD, respectively) and to form inclusion complexes with 1,8-dimethoxymethylnaphthalene (oNy), a model for the cap moiety. The inclusion capacity was further examined against sodium 1-adamantanecarboxylate (AC). Molecular mechanics (MM) and molecular dynamics (MD) calculations in vacuo and in the presence of water were employed to identify the conformational preferences of the isolated Nm α - and Nm γ CDs and the geometry of the resulting dimers. The present work also compares the results for Nm α - and Nm γ CDs with those obtained for Nm β CDs, highlighting the importance of the macroring size in their conformational and self-aggregation behavior. We also have a special interest in contrasting the results with those previously obtained for the xylylene CD

counterparts (Xm CDs)^{68–70} and in further discussing how the size of the double-linked aromatic cap affects the conformational equilibrium and the stabilization of the dimer species.

■ EXPERIMENTAL SECTION

Materials and Experimental Methods. The new naphthalene-capped CDs $Nm\alpha$ CD and $Nm\gamma$ CD were prepared in two steps (Scheme S1 of the Supporting Information) from the corresponding xylylene-capped analogues $Xm\alpha$ CD and $Xm\gamma$ CD by (i) removal of the aromatic group by hydrogenolysis and (ii) reaction of the resulting diols (di-OH $m\alpha$ CD and di-OH $m\gamma$ CD, respectively) with α,α' -dibromo-1,8-dimethylnaphthalene. Removal of the xylylene group in $Xm\alpha$ CD and $Xm\gamma$ CD by Pd-catalyzed hydrogenolysis proceeded smoothly in the presence of formic acid to provide the key diol precursors di-OH $m\alpha$ CD and di-OH $m\gamma$ CD, which upon reaction with α,α' -dibromo-1,8-dimethylnaphthalene afforded the target double-linked naphthalene-capped cyclodextrins $Nm\alpha$ CD and $Nm\gamma$ CD in good yield. Their structure was confirmed by NMR, MS, and microanalytical data. Further details of procedures, general reaction conditions, and relevant spectroscopic data are shown in the Supporting Information.

The Nm CD dilute solutions used in this study for fluorescence and circular dichroism studies were prepared by weight in Milli-Q deionized water and stirred for ~24 h prior to measuring. The concentrations ranged from 0.005 to 5.0 mM (0.006 to 5.4 mM). For the aqueous solution of both m CDs, the range was wider, reaching concentrations as high as 11 mM. All the organic solvents used in the fluorescence and circular dichroism experiments were spectroscopic or purity >98% grade. Nevertheless, they were always checked before use for any fluorescence. 2,3-Butanedione (diacetyl, Aldrich) was used as a fluorescence quencher for the naphthyl group. As a way to prove the accessibility to the CD cavities in solution and the dimer stability, sodium 1-adamantanecarboxylate (AC) (Aldrich) was used. Cylindrical quartz 2 mm inner path cells of 120 μ L capacity were used for most of the experiments. However, for some of the checking, typical rectangular (square cross section) quartz 1 cm path cells were used.

NMR experiments were performed at 500 (125.7) MHz using a Bruker DRX500 instrument in $CDCl_3$ and D_2O . 1-D TOCSY as well as 2-D COSY and HMQC experiments were carried out to assist in signal assignment. 2-D NOESY experiments in D_2O were recorded using a conventional pulse program. The mixing time was fixed at 0.6 s, while TD1 and TD2 were set up to 1024 and 256, respectively.

The absorbance measurements were performed on an UV-visible dual beam Lambda 35 Perkin Elmer spectrophotometer.

The steady-state fluorescence measurements were carried out by using a high sensitivity spectrofluorimeter, the SLM 8100C Aminco, equipped with a cooled photomultiplier and a double (single) monochromator in the excitation (emission) path. Excitation and emission slit widths were selected at 8 nm for both channels. Polarizers were set at the magic angle conditions. More details about the apparatus and conditions were described elsewhere.⁶⁶

Fluorescence intensity correction (I_{corr}) for the inner-filter effect was achieved by

$$I_{corr} = I_{obs} \text{ antilog} \left(\frac{A_{ex} + A_{em}}{2} \right) \quad (1)$$

where A_{ex} and A_{em} are the absorption at the wavelength of excitation and emission, respectively.

The fluorescence decay measurements were achieved on a Time Correlated Single Photon Counting (TCSPC) FL900 Edinburgh Instruments Spectrometer with a thyratron-gated lamp filled with H_2 . Right angle geometry and cylindrical quartz 2 mm inner path cells of 120 μ L capacity were used for most of the experiments. Further details are described elsewhere.⁶⁶

Decay intensity profiles were fitted to a sum of exponential decay functions as

$$I(t) = \sum_{i=1}^n A_i e^{-t/\tau_i} \quad (2)$$

by the iterative deconvolution method.⁷¹ The average lifetime of a multiple-exponential decay function was then defined as

$$\langle \tau \rangle = \frac{\sum_{i=1}^n A_i \tau_i^2}{\sum_{i=1}^n A_i \tau_i} \quad (3)$$

where A_i is the pre-exponential factor of the component with a lifetime τ_i of the multiexponential function intensity decay.

The fractional contribution f_i of each decay time to the steady-state intensity, which represents the fraction of total fluorescence intensity I of the i -component at the wavelengths of observation, is given by

$$f_i = \frac{A_i \tau_i}{\sum_{i=1}^n A_i \tau_i} = \frac{I_i}{\sum_{i=1}^n I_i} \quad (4)$$

and the intensity weighted average lifetime $\langle \tau \rangle$ from a dilute solution of a pair of emitting species, 1 and 2, that do not interact during the excited state lifetime can be obtained as

$$\langle \tau \rangle = f_1 \tau_1 + f_2 \tau_2 \quad (5)$$

For a single isolated excited chromophore which is dynamically quenched by a quencher Q, the τ_0/τ ratio (with/without Q) is related with [Q] by the linear Stern–Volmer equation. For more complicated systems, the Stern–Volmer representations of $\langle \tau \rangle_{q=0}/\langle \tau \rangle$ are linear at the lowest [Q] region.⁷²

The circular dichroism spectra were obtained by using a JASCO-715 spectropolarimeter. Recorded spectra were the average of two scans taken at a speed of 20 nm·min⁻¹ with 0.25 s time response. The sensitivity and resolution were fixed at 20 mdeg and 0.5 nm, respectively. All measurements were performed at 25 °C in cells whose lengths range from 0.1 to 10 cm.

Computational Details. Molecular mechanics (MM) and molecular dynamics (MD) calculations were performed with Sybyl-X 1.2⁷³ and the Tripos Force Field.⁷⁴ A relative permittivity of $\epsilon = 3.5$ ($\epsilon = 1$) was used in the vacuum (in the presence of water). Charges for Nm CDs were obtained by MOPAC.⁷⁵ Structure optimizations were carried out by the simplex algorithm, and the conjugate gradient was used as a termination method with gradients of 0.2 (0.5) kcal mol⁻¹ Å⁻¹ for the calculations carried out in a vacuum (water).^{76,77} Nonbonded cutoff distances were set at 8 Å. For calculations in water, the Molecular Silverware algorithm (MS)⁷⁸ was used for solvation with periodic boundary conditions (PBC) in a canonical (NTV) ensemble. Further details about the theoretical simulations were described previously.⁶⁶

RESULTS AND DISCUSSION

NMR Spectra. The $Nm\alpha CD$ and $Nm\gamma CD$ exhibited remarkable differences in their 1H NMR spectra when recorded in D_2O and in $CDCl_3$ (see Figures S5, S6, S9, and S10 in the Supporting Information). In general, larger chemical shift dispersions were observed in D_2O for the aromatic protons, the cyclooligosaccharide protons, and the methyl signals, whereas the signals for the methylene groups involved in the hinge-type cyclic diether linkage broadened and experienced high field shifts. Those observations suggest that changes in the conformational properties and/or in the aggregation state of the compounds are occurring in water solution, analogously to that encountered in the $XmCD$ series.^{68–70} Interestingly, 1H NMR signal splitting in D_2O is much larger for $Nm\alpha CD$ as compared with $Nm\gamma CD$, suggesting that the double-linked naphthalene group is less mobile in the former. This scenario is consistent with a higher contribution of aggregated species, in which the aromatic ring will be confined to a reduced space, shielded from the solvent, in water solutions of the γCD derivative. Solubility limitations and the fact that in both cases the aqueous solutions exhibited negative temperature coefficients, precipitating upon heating, prevented dynamic NMR experiments at variable concentration and temperature. Spatial correlation (NOESY) experiments discarded the inclusion of the naphthalene moiety in the CD cavity in both compounds. Only cross-peaks between aromatic resonances and secondary rim methoxyls and benzylic methylene hinges were observed in both cases (see Figures S11 and S13 in the Supporting Information), in agreement with what was reported for the $Nm\beta CD$ analogue.⁶⁶ Neither self-inclusion, anticipated to be unfavorable from previous data for the corresponding xylylene adducts,^{68–70} nor intermolecular inclusion complex formation seem to play a relevant role in the corresponding conformational/aggregation equilibria. However, fluorescence and circular dichroism techniques were instead implemented to investigate the conformational/aggregation behavior of these molecules.

Absorption Spectra. The absorption spectra of $Nm\alpha CD$ and $Nm\gamma CD$ in water solution are quite similar and match that recorded for the oNy model compound, which in turn is similar to other naphthalene derivates,^{79,80} but with maxima that are slightly shifted to the blue by about 4 nm. As a representative example, the UV-vis spectrum of $Nm\gamma CD$ in water is shown in Figure 2. It exhibits two intense main bands whose maxima are placed at 220 and 290 nm and a very faint one located at 320 nm. These bands can be ascribed to the 1B_b , 1L_a , and 1L_b electronic transitions, according to Platt's notation.⁸¹ These transition dipole moments are nearly parallel to the long (1B_b) and short (both 1L_a and 1L_b) naphthalene main axis.⁸²

Fluorescence Measurements. Emission Spectra. The emission spectra of $Nm\alpha CD$ and $Nm\gamma CD$ in water are shown in Figure 3. Spectra were obtained upon excitation of the naphthalene group at 295 nm, and they exhibit a double band located at ~335 and ~342 nm and a shoulder at ~355 nm. None of the spectra exhibited emission from naphthalene excimers.

The association constant K_D for the dimerization process of $NmCD$ described by the equilibrium

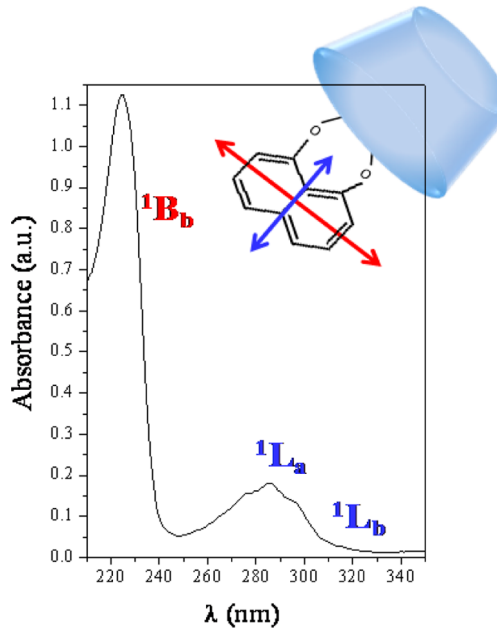


Figure 2. Absorption spectra for $Nm\gamma CD$ in dilute water solution at 25 °C. Superimposed is the $NmCD$ structure showing the directions of the electronic transition moments.

can be related to the fluorescence intensity (I) measured as the area under the naphthyl group emission spectrum and the total $[NmCD]$ by eq 7:⁶⁹

$$I = \frac{\phi_{(NmCD)_2}[NmCD]_0 - (\phi_{(NmCD)_2} - \phi_{NmCD})}{(\sqrt{8K_D[NmCD]_0 + 1} - 1)} \quad (7)$$

where $\phi_{(NmCD)}$ and $\phi_{(NmCD)_2}$ are the proportionality constants (per chromophore unit) between the fluorescence intensity and concentration of the monomer and dimer form, respectively.

As shown in Figure 3, an I_{corr} vs $[NmCD]_0$ linear behavior and a constant $I_{corr}/[NmCD]_0$ ratio in the whole range of $NmCD$ concentrations were observed for both types of $NmCDs$ at 25 °C. This means (eq 7) that the fluorescence quantum yield does not change during the dimerization process and $\phi_{NmCD} \approx \phi_{(NmCD)_2}$. The same behavior is observed for all the temperatures (5–45 °C). This fluorescence intensity response was also observed for $Nm\beta CD$ ⁶⁶ and $XmCDs$.^{68–70}

Fluorescence Intensity Decays. Fluorescence decay profiles for $Nm\alpha CD$ and $Nm\gamma CD$ in water solutions at different $[NmCD]$ and temperatures were performed at the maximum of the emission band (342 nm) upon 295 nm of excitation. Emission profiles were fitted to the sum of three-exponential decays at any $[NmCD]$ and temperature. The short-lived component (~0.2 ns) was ascribed to the innate stray light and/or scattering of the cylindrical cuvettes used. The intermediate (~12 ns) and slowest (~30 ns) components were assigned to the free ($NmCD$) and the dimer ($NmCD$)₂ species, respectively. A similar conduct was observed for the $Nm\beta CD$,⁶⁶ as well as their $XmCD$ counterparts.^{69,70}

The influence of the $NmCD$ concentration on the lifetime component contributions (eq 4) was analyzed in Figure 4. The fraction of the intermediate (large) component corresponding to the monomer (dimer), f_{NmCD} ($f_{(NmCD)_2}$), for any of the three $NmCDs$, decreased (increased) as the concentration increased.

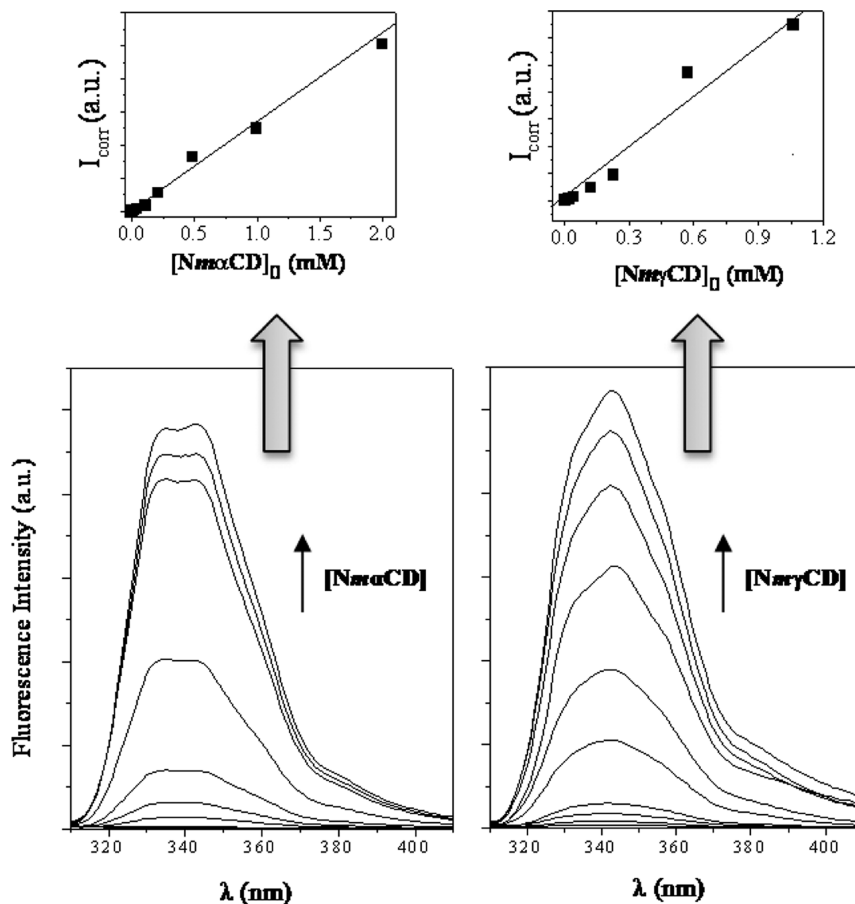


Figure 3. (upper) Variation of the corrected fluorescence intensity I_{corr} as a function of the $[N\text{mCD}]_0$. (bottom) Emission spectra for Nm α - and Nm γ CD/water solutions at different $[N\text{mCD}]_0$ (mM) at 25 °C.

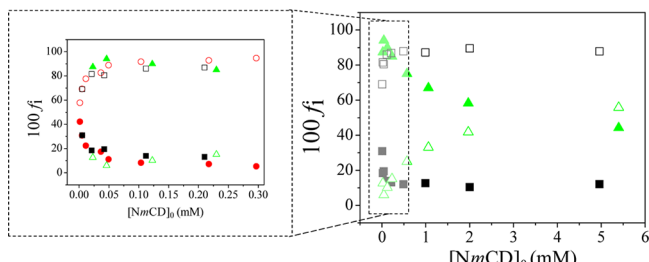


Figure 4. Variation in the fractions of dimer, $f_{(NmCD)_2}$ (open symbols), and monomer, f_{NmCD} (filled symbols), with the $[NmCD]_0$: Nm α CD (□), Nm β CD (○), and Nm γ CD (△). Data for Nm β CD were obtained from ref 66.

However, as shown in Figure 4, the variation of this ratio with concentration exhibited very different trends in quantitative terms, for Nm α - and Nm γ CD, probably derived from differences in the respective K_D values. For Nm α - (as for Nm β CD⁶⁶), K_D had to be very large, since virtually 100% of the fraction of the dimer was reached at very low concentrations ($[NmCD] > 0.10$ mM). Even at the lowest concentrations, the fraction of the dimer was higher than the monomer. On the contrary, $f_{Nm\gamma\text{CD}}$ at low concentrations was larger than $f_{(Nm\gamma\text{CD})_2}$ and it hardly varied with $[Nm\gamma\text{CD}]$ in the 0–0.30 mM range. However, at higher concentrations (in the 0.30–6 mM range), $f_{Nm\gamma\text{CD}}$ ($f_{(Nm\gamma\text{CD})_2}$) monotonically decreased (increased) and the

fraction of the dimer almost reached 0.5. Surely, this will result in a much lower K_D for Nm γ CD than for the other NmCDs.

Thermodynamics of the Dimerization Processes. Figure 5 shows an increase in $\langle \tau \rangle$ (obtained from eq 3) with $[NmCD]$ for the new naphthalene-capped CDs, as a result of the increase in dimer fraction. For Nm α CD, a constant value of $\langle \tau \rangle$ was reached at low concentrations; however, for Nm γ CD, the curve was much less pronounced. This result also points to a much lower K_D for this latter system.

Experimental values of the weighted average lifetimes, $\langle \tau \rangle$, as a function of $[NmCD]$ from Figure 5 were adequately fitted to the following equation⁶⁹

$$\langle \tau \rangle = \frac{2\tau_{NmCD} + (\phi_{(NmCD)_2}/\phi_{NmCD})\tau_{(NmCD)_2}(\sqrt{8K_D[NmCD]}_0 + 1 - 1)}{2 + (\phi_{(NmCD)_2}/\phi_{NmCD})(\sqrt{8K_D[NmCD]}_0 + 1 - 1)} \quad (8)$$

under the $\phi_{(NmCD)_2}/\phi_{NmCD} = 1$ assumption. In the calculation of $\langle \tau \rangle$ values derived from eq 8 and depicted in Figure 5, the fastest component (arising from light scattering) was not taken into account. Table 1 collects the dimerization constants and the values of τ_{NmCD} and $\tau_{(NmCD)_2}$ for the different types of NmCDs at several temperatures.

The K_D values obtained for Nm γ CD were higher in comparison with those for similar naphthalene-substituted γ CDs.⁸³ Something similar occurred for Nm β CD when it was compared to other naphthalene- β CDs.^{84,85} As far as we know, dimerization constants for naphthalene- α CDs were not reported before. K_D values in water for Nm α - and - β CDs

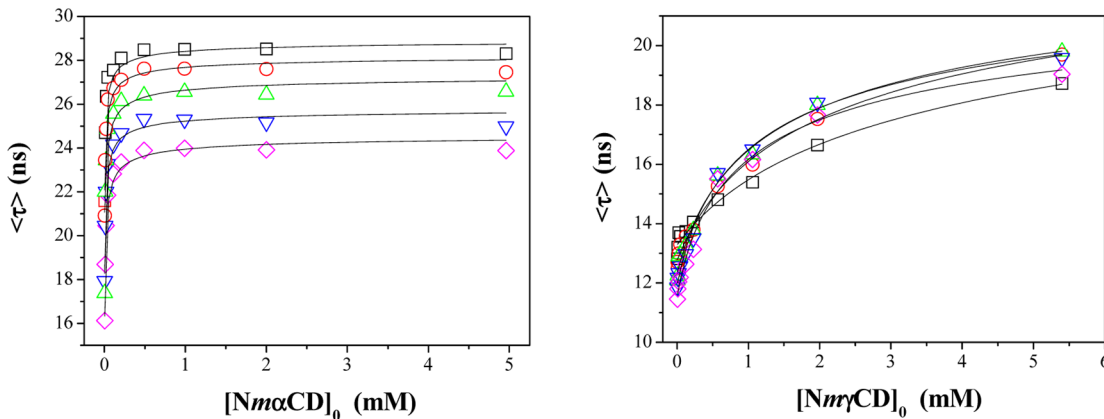


Figure 5. Variation of the average lifetime ($\langle \tau \rangle$) as a function of $[NmCD]_0$ for aqueous solutions of $Nm\alpha$ CD (left) and $Nm\gamma$ CD (right) at different temperatures: 5 °C (□); 15 °C (○); 25 °C (△); 35 °C (▽); 45 °C (◇).

Table 1. Dimerization Constants K_D , τ_{NmCD} , and $\tau_{(NmCD)_2}$ Parameters Obtained from the Fluorescence Decay Profiles at Five Temperatures for $Nm\alpha$ CD and $Nm\gamma$ CD/Water

Nm α CD			
T (°C)	$10^{-5} \times K_D$ (M $^{-1}$)	$\tau_{Nm\alpha CD}$ (ns)	$\tau_{(Nm\alpha CD)_2}$ (ns)
5	7.4 ± 2.8	6 ± 37	29.1 ± 0.4
15	6.8 ± 1.7	5 ± 24	28.2 ± 0.3
25	7.8 ± 3.0	3 ± 52	27.4 ± 0.6
35	5.1 ± 9.2	4 ± 16	25.9 ± 0.3
45	4.2 ± 6.2	2 ± 13	24.7 ± 0.3
Nm γ CD			
T (°C)	K_D (M $^{-1}$)	$\tau_{Nm\gamma CD}$ (ns)	$\tau_{(Nm\gamma CD)_2}$ (ns)
5	130 ± 40	13.2 ± 0.1	25.4 ± 1.8
15	240 ± 45	12.6 ± 0.1	25.5 ± 0.9
25	400 ± 85	12.3 ± 0.1	24.4 ± 0.8
35	510 ± 90	12.0 ± 0.1	23.8 ± 0.7
45	580 ± 130	11.5 ± 0.1	22.9 ± 0.7

were much larger (~ 3 orders of magnitude) than for their Xm CD analogues.^{69,70} $Nm\gamma$ CD and $Xm\gamma$ CDs, however, were of the same magnitude order, exhibiting quite similar K_D values around ~ 400 and ~ 250 M $^{-1}$ at 25 °C, respectively. This indicates that not only does the macroring size influence the dimer stability of secondary face, double-linked capped CDs, but the chromophoric cap group size also plays an important role. Thus, the bigger size of the naphthalene moiety as compared with xylylene seems to contribute to enhance the dimer stabilization in the α CD and β CD series, but this effect is virtually canceled in the case of the larger γ CD platform.

The ΔH^0 and ΔS^0 values for the dimerization equilibria could be obtained from the change of K_D with temperature. Despite the uncertainties accompanying K_D values, innate from the experimental method, van't Hoff plots were reasonably linear (Supporting Information, Figure S15) over the whole temperature range studied. Thermodynamic parameters are listed in Table 2.

The dimerization process for $Nm\alpha$ CD was exothermic, as was the case for the $Nm\beta$ CD homologue.⁶⁶ This scenario is similar to that encountered for the corresponding xylylene-capped counterparts Xm CDs^{68,69} and is related to association processes which are favored by van der Waals and/or electrostatics attractive interactions.^{31,86} In stark contrast, $Nm\gamma$ CD dimerization is endothermic, probably because these

Table 2. ΔH^0 and ΔS^0 of the Dimerization Processes for the Three Types of Nm CD's

system	ΔH^0 (kJ·mol $^{-1}$)	ΔS^0 (J·K $^{-1}$ ·mol $^{-1}$)
$Nm\alpha$ CD	-10.1 ± 3.9	$+77 \pm 13$
$Nm\beta$ CD ^a	-21.3 ± 2.7	$+25 \pm 9$
$Nm\gamma$ CD	$+27.0 \pm 3.6$	$+139 \pm 12$

^aData extracted from ref 66.

attractive interactions are weaker due to the increased size and flexibility of the γ CD macrocycle.^{87,88}

Dimerization of the three Nm CDs was characterized by favorable entropy changes ($\Delta S^0 > 0$), which is opposite to that observed for the corresponding Xm CDs.^{68,69} The larger size and higher hydrophobic nature of the naphthalene, as compared to xylylene, must be responsible for the change in ΔS^0 sign. The loss of order that accompanies the rupture of the hydration water shells of the naphthalene moiety during Nm CD dimerization, much greater than in the case of the xylylene segment in Xm CDs, is probably responsible for the observed differences in the thermodynamic signatures.

Fluorescence Quenching by Diacetyle. The large disparity in K_D values for $Nm\alpha$ CD and $Nm\gamma$ CD prevented quenching experiments at the same dimer fraction. Instead, parallel measurements were carried out at two rather different Nm CD concentrations: 0.26×10^{-2} and 0.26 mM. Dimer fractions at $[NmCD]_0 \approx 0.26 \times 10^{-2}$ mM (≈ 0.26 mM) were 0.44 (0.91) and ~ 0 (0.08) for $Nm\alpha$ - and γ CD, respectively.

The Stern–Volmer representations of $\langle \tau \rangle_{q=0}/\langle \tau \rangle$ were linear over the whole concentration range of diacetyle (0–0.1 M). The bimolecular constants, k_q , at 25 °C for the model compound oNy and for the Nm CDs at the two concentrations studied are collected in Table 3.

As expected, the naphthalene chromophore was found to be less accessible when attached to the macroring in Nm CDs at the two concentrations studied than when it was free (oNy). An increase in the Nm CD concentration resulted in a dimer fraction increase and concomitant k_q decrease. These data are compatible with the shielding of the naphthalene chromophore in a sandwich-type architecture (HH dimer), or in a stacked arrangement (HT dimer) upon aggregation, thereby substantially hindering the quencher access to the naphthalene moiety. Nevertheless, even at $[Nm\gamma CD]_0 = 0.26 \times 10^{-2}$ mM, with almost 100% of the capped cyclodextrin derivative in the monomer form, a $k_q(Nm\gamma CD) < k_q(oNy)$ relationship was

Table 3. Bimolecular Quenching Constant, k_q ($\times 10^{-9} \text{ M}^{-1} \text{ s}^{-1}$), for $Nm\alpha\text{CD}$, $Nm\beta\text{CD}$, $Nm\gamma\text{CD}$, and oNy in Water at 25°C

$[Nm\text{CD}]_0$	k_q ($\times 10^{-9} \text{ M}^{-1} \text{ s}^{-1}$)			
	$Nm\alpha\text{CD}$	$Nm\beta\text{CD}^a$	$Nm\gamma\text{CD}$	oNy
0.26 mM	0.11 ± 0.01	0.09 ± 0.01	0.48 ± 0.03	
0.26×10^{-2} mM	1.7 ± 0.4	1.6 ± 0.5	2.4 ± 0.2	3.0 ± 0.2

^aData obtained from ref 66.

observed. This fact implies that the accessibility of the naphthalene cap in $Nm\gamma\text{CD}$ monomer species is also smaller than the free oNy. The larger k_q values, whatever the concentration was, obtained for $Nm\gamma\text{CD}$ as compared to $Nm\alpha$ - and βCDs , are related to the large differences in K_D values. Furthermore, the relationship between k_q at high and low concentrations follows the K_D trend; i.e., the variation of k_q with the concentration is much larger for $Nm\alpha\text{CD}$ and $Nm\beta\text{CD}$ ⁶⁶ (~16-fold between the two concentrations) than $Nm\gamma\text{CD}$ (only ~5-fold).

Effect of the Medium Polarity (ϵ) and Microviscosity (η) in the Dimerization Process. The nonvariation in the fluorescence quantum yields (ϕ) and the increase in the weighted average lifetimes ($\langle\tau\rangle$) during aggregation can be associated with the polarity (ϵ) and microviscosity (η) changes that the naphthalene chromophore experiences upon dimer formation. To have a deeper insight into those aspects, the effect of the solvent polarity and microviscosity on the fluorescence properties of oNy, as a model compound of the appended naphthalene group, was assessed.⁶⁶ In brief, τ for oNy showed its maximum value for $\epsilon \approx 50$ to slightly (drastically) decrease for $\epsilon > 50$ ($\epsilon < 50$), whereas it increased with η . By contrast, ϕ almost remained independent of ϵ and η ($\phi = 0.08 \pm 0.06$). From this data, it can be inferred that the dimerization process must involve a decrease in the polarity of the medium surrounding the appended moiety, from nearly the value for bulk water ($\epsilon \approx 78$) to a medium confined between two CD platforms (probably $\epsilon \geq 50$), and an apparent increase in η at the chromophore surroundings. This fact will agree with our experimental findings, where $\phi_{(Nm\text{CD})_2} \approx \phi_{Nm\text{CD}} = 1$ and $\tau_{(Nm\text{CD})_2} > \tau_{Nm\text{CD}}$.

The influence of the medium polarity on the dimerization processes was also investigated from the analysis of the fluorescence intensity decay profiles for NmCD dilute solutions ($[Nm\text{CD}] = 0.2$ mM) in several solvents at 25 °C. At this concentration, the $Nm\alpha\text{CD}$ ($Nm\gamma\text{CD}$) dimer fraction in water was 0.90 (0.07). Figure 6 shows a decrease in both the ratio of dimer-to-monomer fractions (eq 4) and $\langle\tau\rangle$ when the polarity of the solvent decreases. This observation indicates a displacement of the equilibria toward the monomeric species, whose lifetime component is faster. The less polar medium most likely weakens the hydrophobic interactions between CDs, leading to a rupture of the dimer. As a consequence of the low K_D values, the variation of both parameters, depicted in Figure 6, is less significant for $Nm\gamma\text{CD}$.

To get a deeper understanding of the interactions involved in dimer formation, we investigated the effect of a strong guest competitor, namely, 1-adamantanecarboxylate (AC), in the self-assembling equilibria. The addition of AC to 0.2 mM solutions of the previously reported $Nm\beta\text{CD}$ (in different solvents), up to AC concentrations near 1.6 mM, did not produce any change in any of the parameters depicted in Figure 6.⁶⁶ Experiments performed at other $[Nm\beta\text{CD}]$ or temperatures (25 and 45 °C) led to similar results.

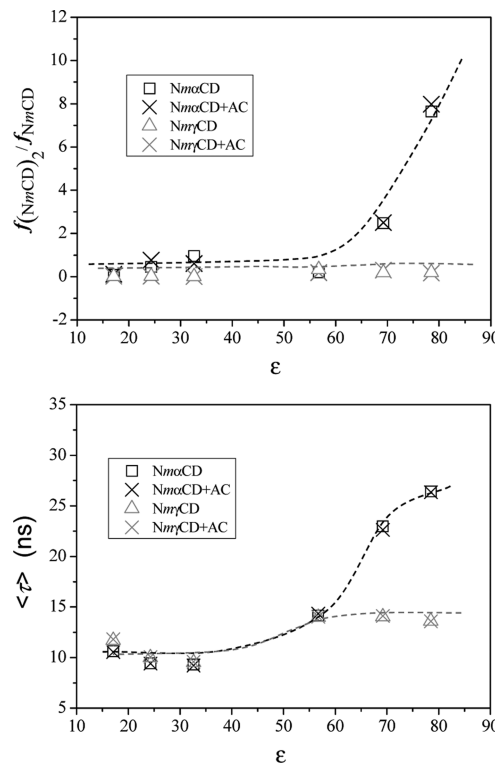


Figure 6. Variation of the ratios of the dimer-to-monomer fraction (upper) and the average lifetime $\langle\tau\rangle$ (bottom) as a function of ϵ , for $Nm\alpha\text{CD}$ and $Nm\gamma\text{CD}$ different solutions at 25 °C in the absence and in the presence of 1-adamantanecarboxylate (AC). The solvents were water, methanol:water v/v mixtures (20:80, 50:50), ethanol, and butanol.

Although the affinities of adamantane derivatives with α - and with γCDs are much lower than those for βCD ,^{89–91} AC was also added to each $Nm\alpha$ - and $Nm\gamma\text{CD}$ solution of different solvents up to reaching 8-fold excess. As depicted in Figure 6, no change in the equilibrium in the presence of AC was apparently observed again, whatever the solvent and the NmCD used. The results should be interpreted with caution, as the absence of any change could probably be attributed to the strength of the interactions stabilizing the dimers (for $Nm\alpha$ - and $Nm\beta\text{CD}$) but also to the fact that the bulky naphthalene cap might hinder the formation of the AC complex with the monomer or that its complexation constant is very low. This must be the dominant effect at least for the γCD derivative, $Nm\gamma\text{CD}$, since at the concentration used in water the monomer represents 93% of the total $Nm\gamma\text{CD}$ molar concentration.

Study of the Heterodimerization Process. Investigation of heteroassociation processes of NmCDs with the permethylated $m\text{CD}$ partners, lacking the aromatic moiety, and evaluation of the inclusion capabilities of the later toward the oNy model were carried out in order to assess the role of the naphthalene (Ny) group in the self-assembling properties of NmCDs (Supporting Information, Figure S16).

Experiments carried out at constant $[NmCDs]$ (≈ 0.02 mM), by changing the $[mCD]$, evidenced no substantial change in $\langle\tau\rangle$ for the $Nm\alpha CD/m\alpha CD$ system. At the $[Nm\alpha CD]$ used, about 72% of $Nm\alpha CD$ was in the dimer form, and even after addition of a great excess of $m\alpha CD$ ($\sim 400 \times [Nm\alpha CD]$), the $(Nm\alpha CD)_2$ species did not dissociate. No evidence of formation of hybrid dimers was observed, similarly to that previously encountered for $Nm\beta CD$ and $m\beta CD$.⁶⁶ These results reinforce the idea that the direct interaction of the two aromatic groups in the dimer components is primarily responsible for the high stability of the dimer species, as it was the case for double-linked xylylene-capped derivatives $XmCDs$.^{69,70} The most plausible orientation of the CD units in the dimer is, then, the head-to-head type (HH). In contrast, the decreasing trend in $\langle\tau\rangle$ value with $[m\gamma CD]$ for the $Nm\gamma CD/m\gamma CD$ system is ascribable to the formation of heterodimers. In this case, at the $[Nm\gamma CD]$ used, almost 99% was in the monomer form. This would also point toward the possibility of the formation of stable HT-type dimers for $Nm\gamma CD$, as it was also observed in the case of $Xm\gamma CD$.⁷⁰

Solutions of oNy ($\sim 10^{-2}$ mM) in water did not exhibit any noticeable change in $\langle\tau\rangle$ in the presence of different $m\gamma CD$ concentrations, as occurred with $m\beta CD$.⁶⁶ oNy does apparently not form any complex with $m\gamma CD$, or if it does, the complexation constant should be very low. On the contrary, a monotonic increase in $\langle\tau\rangle$ with $[m\alpha CD]$ was observed. This may indicate that the $m\alpha CD$ has an optimum cavity size, or that the intermolecular interactions are favorable for the $oNy/m\alpha CD$ complex formation. This interaction could also explain the large stability of the $(Nm\alpha CD)_2$ dimers. However, it must be pointed out that the Ny group is attached to the $Nm\alpha CD$ macrocycle as a hinge by two relatively short chains. Therefore, the HH association of two $Nm\alpha CDs$ might not imply the mutual inclusion of Ny in their neighbor CD cavities due to the strong steric hindrance of the macrocycles on approaching. Nevertheless, this will be dealt with in more detail in the computational simulation section, later in this manuscript.

Circular Dichroism Measurements. The induced circular dichroism (ICD) spectrum intensity and sign varies depending on the depth of the chromophore inclusion, its fitting in the CD cavity, and the orientation of its electronic transition moment relative to the CD *n*-fold axis. Parallel (perpendicular) orientation gives a positive (negative) ICD band, which becomes the opposite sign when the chromophore is located partially outside.^{82,92,93} The effect of the medium polarity (the same solutions as those used in the section Effect of the Medium Polarity and Microviscosity in the Dimerization Process) on ICD spectra covering the 1B_b and 1L_a (or 1L_b) absorption band regions for $NmCDs$ is shown in Figure 7. The ICD spectra for the $Nm\alpha CD$ water solution (0.2 mM, 90% of dimer) exhibited exciton coupling (EC) signals at both 1B_b and 1L_a (or 1L_b) regions. The intensity of the signals decreased as the medium polarity decreased, from water to 20% methanol:water mixture. For less polar solvents, both EC signals disappeared, becoming single bands. Something similar occurred for the $Nm\beta CD$, even though it was only in the 1B_b region.⁶⁶ These results, which support HH dimer structures, certainly indicate that in the high polar solvents the two Ny chromophores are close in space. However, when the environment turns more hydrophobic, the interaction between Ny groups becomes weaker, shifting the equilibrium toward the monomer species. Similar conclusions were reached by fluorescence experiments (Figure 6). In addition, this would

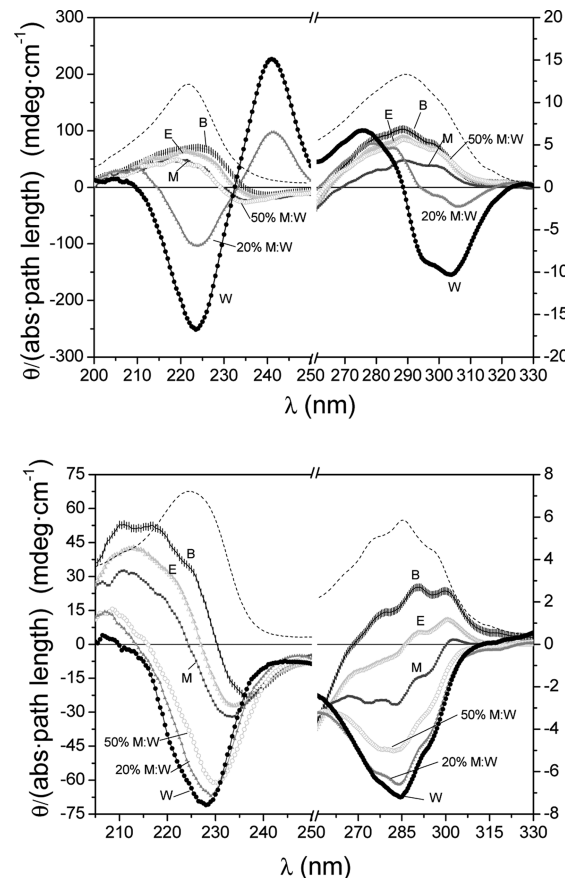


Figure 7. ICD spectra for $Nm\alpha CD$ (upper) and $Nm\gamma CD$ (bottom) solutions ($[NmCD] \approx 0.2$ mM) in different polarity solvents at 25 °C. The solvents were water (W), methanol:water v/v mixtures (20 and 50% M:W), methanol (M), ethanol (E), and butanol (B).

also agree with the fact that the dimerization processes of the $NmCD$ in water were accompanied by $\Delta S^0 > 0$, where the hydrophobic effect plays a key role in polar media.

ICD spectra for $Nm\gamma CD$ /water solution (0.2 mM, ~7% of dimer), however, did not exhibit EC signals. Instead, it showed two negative bands whose intensity decreased and became positive in highly nonpolar solvents. According to the rules of Kodaka,^{82,92,93} the negative signs would be in agreement with an HT dimer where Ny is located inside or strongly interacts with the cavity and both transition moments are perpendicular to the main axis of the macrocycle. The formation of heterodimers in the presence of $m\gamma CD$ would also agree with this fact. Something similar happened in the case of the analogue $Xm\gamma CD$, where the HT approximation was also favorable.⁷⁰

It is interesting to point out that the three $NmCD$ systems have ICD spectra that are quite similar in high nonpolar solvents: a relatively strong positive band for the 1B_b transition and an also positive but much weaker band for the 1L_a one. These signals would agree with the presence of a monomeric species, with a similar structure for the three $NmCD$ macrocycles, where naphthalene is located outside the cavity with its long axis oriented perpendicular to the main CD axis and the short axis relatively displaced from this perpendicularity to the cavity.^{82,92,93} No changes in the ICD spectra were observed for any of the $NmCD$ and solvents used upon AC addition, corroborating the results obtained by fluorescence experiments depicted in Figure 6.

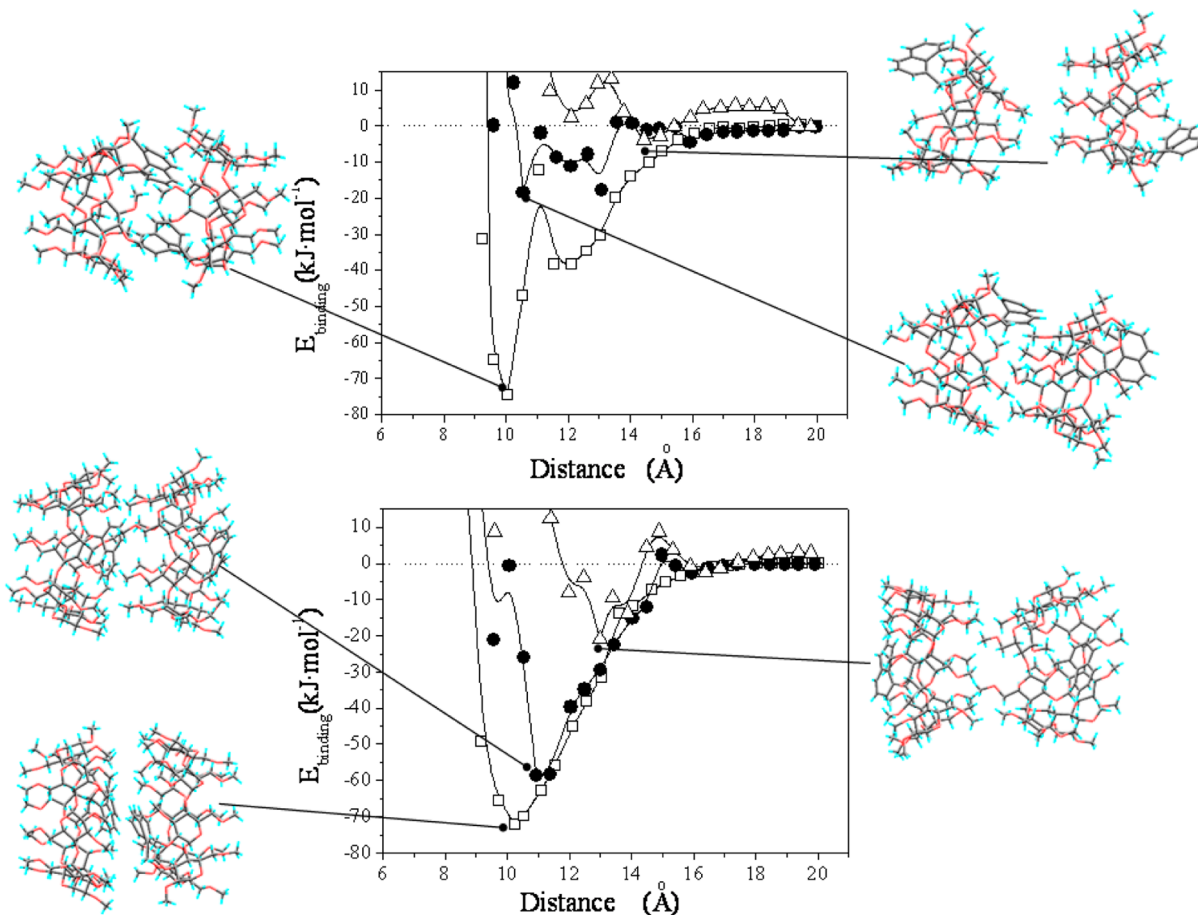


Figure 8. Changes in the binding energies when a second $NmCD$ (y coordinate in \AA) by HH (□), HT (●), and TT (△) orientations for the $Nm\alpha CD$ (upper) and $Nm\gamma CD$ (bottom). Superimposed are the MBE ($NmCD$)₂ structures.

Theoretical Studies: Molecular Mechanics and Molecular Dynamics. Conformational Study of $NmCD$. The probability distribution for several distances and angles of the macrorings for the isolated $NmCD$ was obtained from the analysis of molecular dynamics 10 ns trajectories in vacuo at different temperatures. As starting structures for the MD simulations of $Nm\alpha$ - and $Nm\gamma$ CDs, the four torsional angles by rotation around the bonds that contain the ether groups that link the naphthyl group to the macroring were settled at positions that correspond to the *open* conformation. This conformation, where the naphthyl moiety is placed quasi-perpendicular to the secondary CD rim, is the one that best reproduces the experimental results obtained by fluorescence, circular dichroism, and ^1H NMR for $Nm\beta CD$.⁶⁶

The probability distributions (Supporting Information, Figure S17) for the distance between the centers of mass of the cyclodextrin and the chromophore group (Ny) for $Nm\alpha CD$ and $Nm\gamma CD$ showed just a single maximum at all temperatures, demonstrating the absence of any conformational *open* \rightleftharpoons *capped* equilibrium. This equilibrium was observed for $Xm\alpha$ - and $Xm\beta$ CDs.⁶⁹ The distribution is quite narrow for $Nm\alpha CD$ due to the small macrocycle size and its higher rigidity. Comparing the probability distributions for the three Nm CDs with the K_D values, we can infer that, as the size, flexibility, and conformational freedom of the macrocycle decrease, the K_D values increase.

The distributions of the angles between the main macroring axis and the directions of the electronic transition moments $^1\text{B}_b$

and $^1\text{L}_a$ (Supporting Information, Figure S18) were also obtained. The average values for the $^1\text{B}_b$ and $^1\text{L}_a$ transitions in $Nm\alpha CD$ ($Nm\gamma CD$) at 600 K were $64 \pm 12^\circ$ ($73 \pm 13^\circ$) and $31 \pm 12^\circ$ ($38 \pm 17^\circ$), respectively. These values are very close to those obtained for $Nm\beta CD$ ($99 \pm 28^\circ$ for $^1\text{B}_b$ and $27 \pm 24^\circ$ for $^1\text{L}_a$).⁶⁶ They also were in good agreement with the conclusions raised by ICD spectra depicted in Figure 7 (two positive bands, strong for $^1\text{B}_b$ and quite weak for $^1\text{L}_a$ or $^1\text{L}_b$) in nonpolar solvents for any of the Nm CDs studied. These facts also support analogous monomer $NmCD$ structures.

Study of the Dimerization Process. Figure 8 depicts the changes in the interaction energy for dimerization processes as a function of the distance along the y coordinate (d , \AA) between the centers of both $Nm\alpha$ - and $Nm\gamma$ CDs for the different HH-, HT-, and TT-type approaches derived from MM calculations. The results indicated that the most favorable approach (structure for the minima interaction energy, MBE) in both cases was the HH type, although the other orientations also provided favorable interaction energies. Nevertheless, the HT approach for $Nm\gamma CD$ was also very stable, providing binding energies that were very close to those for HH arrangements.

Table 4 lists the most significant geometrical parameters, the different contributions to the interaction energies, and those involving naphthalene groups for the different $Nm\alpha$ - and $Nm\gamma$ CDs approaches at the MBE. Except for the TT approach where the Ny–Ny interaction obviously hardly exists, almost all the contributions for both $Nm\alpha$ - and $Nm\gamma$ CDs were favorable. The MBE structures are also superimposed in Figure 8. Such

Table 4. Binding Energy and Other Contributions (kJ mol⁻¹) and Geometrical Parameters for the MBE for N α CD and N γ CD by HH, HT, and TT Approaching, Obtained by MM in the Presence of Water

parameter	N α CD			N γ CD		
	HH	HT	TT	HH	HT	TT
distance CD1–CD2 (Å)	10.0	10.5	14.4	10.3	10.9	13.0
distance Ny1–Ny2 (Å)	6.8	11.4	24.1	3.8	10.7	19.2
θ (deg)	83.5	95.5	66.2	82.8	85.0	56.2
E_{binding}	-74.7	-18.4	-3.9	-72.3	-58.4	-20.9
electrostatics	-31.4	-7.8	9.7	-21.7	-2.7	-7.5
van der Waals	-43.3	-10.6	-13.5	-50.6	-55.7	-13.4
E_{inter} Ny2–NmCD1	-16.5	-0.2	0	-35.2	0	3.8
E_{inter} Ny1–NmCD2	-46.6	11.3	0	-26.3	-0.3	0.5
E_{inter} Ny1–Ny2	-7.0	-0.2	0	-5.3	0	0

structures were optimized and used as starting conformations for the MD simulations.

Figure 9 shows the histories of the binding energies and the distances between centers of mass of each NmCD in the

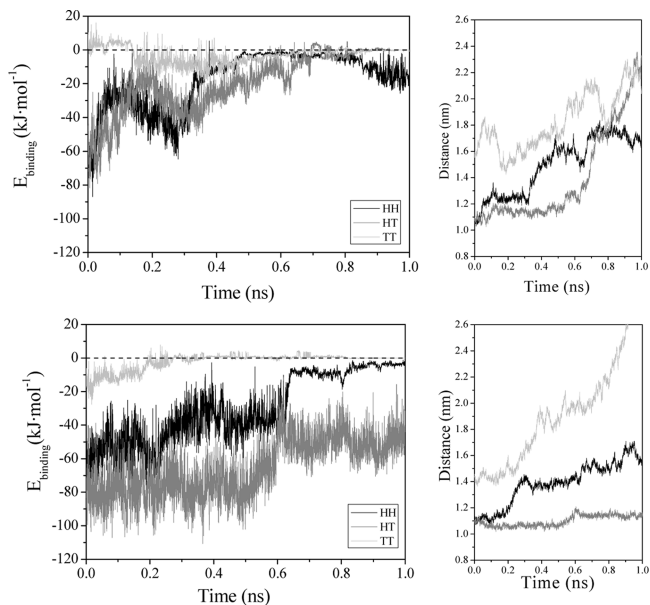


Figure 9. Histories for CD–CD binding energies and center of mass distances for (NmCD)₂ dimers by HH (black), HT (gray), and TT (light gray) orientations starting from the minimized MBE structures obtained from MM calculations for the most stable N α CD (upper panels) and N γ CD (bottom panels) conformations.

(NmCD)₂ dimers obtained from the 1 ns MD analysis in the presence of water at 300 K. In a way similar to the results obtained by MM, the HH approximation for N α CD seems to be the most stable and it does not dissociate after the 1 ns trajectory. In the case of N γ CD, the HH and HT arrangements have favorable interaction energies, although HT is energetically more feasible. By contrast, TT dimers were not stable for any of the NmCDs.

The MBE structures for HH and HT (NmCD)₂ obtained from the MD simulation are shown in Figure 10. This HH–(N α CD)₂ dimer structure supports most of the experimental findings. Ny groups are separated by a distance of about 7–8 Å where the Ny–Ny exciton coupling interactions are favorable.⁹⁴

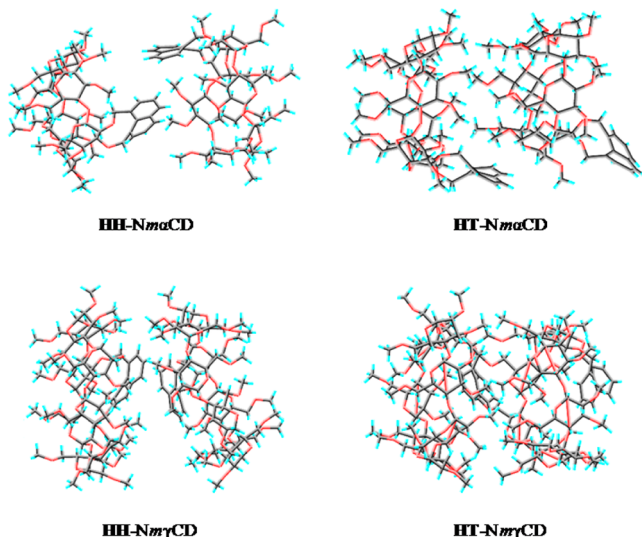


Figure 10. Minima binding energy HH-type (left) and HT-type (right) structures for (N α CD)₂ (upper) and (N γ CD)₂ (bottom) obtained from the analysis of 1 ns MD simulations.

However, the arrangement of naphthalene groups is far from a parallel stacked-type structure capable of forming excimers.

The most favorable approach for the N γ CD dimer is the HT structure shown in Figure 10. For this arrangement, the chromophores are relatively far away from each other and approximately perpendicular to the axis of the CD (parallel to macrocycle) but close to its cavity and the cavity of the neighbor CD (at least one of them), as was predicted from the ICD spectra in high polar solvents.

Since the HT–(N γ CD)₂ is the most stable arrangement, the possibility of the formation of larger supramolecular structures (trimers or oligomers) might be considered. For this purpose, MM and MD calculations were performed on a HT trimer, following the same protocol previously used for the analogous xylene-capped γ CD trimer (X γ CD)₃.⁷⁰

As shown in Figure 11, interactions between the different pairs of adjacent N γ CDs for the trimer (N γ CD)₃ are favorable throughout the whole 1.5 ns MD trajectory. For these arrangements, Ny groups were located approximately parallel (perpendicular) to the macroring (main CD axis) but near its cavity and/or probably the cavity of its neighbor CD. This structure would explain the negative signs for both bands in the ICD spectra of polar solvents. These results contrast with those obtained for X γ CD, whose trimer was found not to be stable.⁷⁰

CONCLUSIONS

The NMR, fluorescence, and circular dichroism results demonstrate that 2¹,3¹-O-(1,8-dimethylnaphthalene- α,α' -diyl)-per-O-methyl- α - and γ -CDs are able to self-aggregate in aqueous dilute solutions. Dimerization constants in water for N α CD (800×10^3 M⁻¹ at 25 °C) and N β CD⁶⁶ (92×10^3 M⁻¹ at 25 °C) were much larger than those obtained previously for their X α CD counterparts, containing xylene instead of naphthalene as capping groups.⁶⁹ The association processes for N α - and N β CD were enthalpy and entropy favored. The $\Delta H^0 < 0$ values are quite similar to those obtained for (X α CD)₂ formation. However, the $\Delta S^0 > 0$ values contrast with the negative ones obtained for X α CDs.⁶⁹ This sign is attributed to the much higher loss of solvation order during

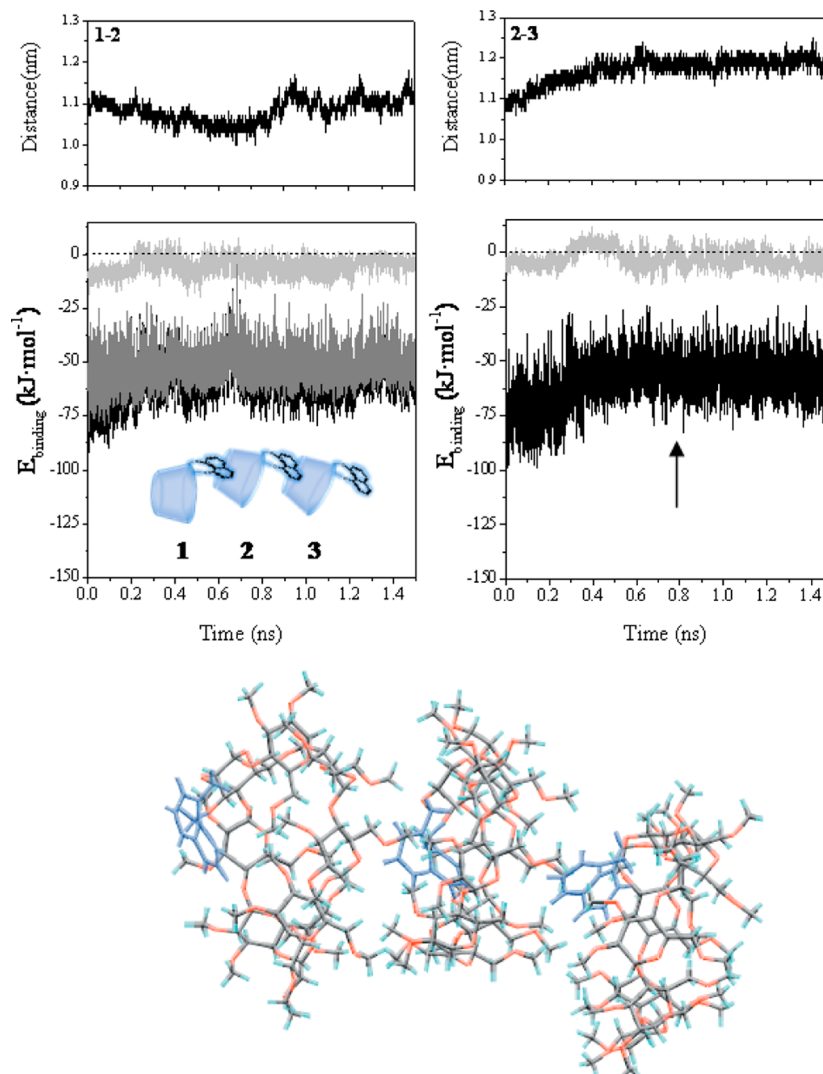


Figure 11. (upper) Histories of interaction energies for HT-type (NmyCD)₃ trimer obtained from the 1.5 ns MD trajectory at 300 K. The interaction energies indicated are total (black), van der Waals (gray), and electrostatics (light gray) contributions. The trajectories are indicated in pairs: 1–2 (left) and 2–3 (right). The structure of the trimer shown (bottom) was obtained after 0.839 ns (indicated by the arrow) and corresponds to the minimum potential energy.

dimerization for the larger naphthyl appended moiety. For the NmyCD , the dimerization constant (401 M^{-1} at 25°C) is significantly smaller than that for $\text{Nm}\alpha$ - and $\text{Nm}\beta\text{CD}$ but remains double as compared with its analogue with xylylene XmyCD .⁷⁰ Although the entropy is $\Delta S^0 > 0$ (as in the other NmCDs), the process is now accompanied by $\Delta H^0 > 0$. Its large macroring size and conformational flexibility are responsible for a weakening in the intermolecular interactions between the CD components in the dimer. For all the NmCDs , dimer formation is more favorable in high polarity solvents. These dimers do not dissociate in the presence of high affinity guests.

The theoretical results supported the absence of any *open ⇌ capped* equilibrium for the $\text{Nm}\alpha$ - and NmyCDs monomer species, as occurred for $\text{Nm}\beta\text{CD}$. The isolated monomers prefer to adopt an open conformation, which is very similar for the three NmCDs , as inferred from the ICD spectra in very nonpolar solvents. The head-to-head-type approaching provides the most stable structures for the $\text{Nm}\alpha$ - and $\text{Nm}\beta\text{CDs}$ dimers, where the naphthalene moieties are relatively close to each other to couple their transition moments, as the EC signal

demonstrates, but without forming excimers. The naphthalene groups are also relatively shielded from the solvent, although they apparently do not penetrate inside the cavity of the neighbor CD. In the case of NmyCD , head-to-tail-type dimer structures are predominant and the presence of associations in head-to-tail trimers and/or oligomers could be energetically favorable. Overall, the reported results provide a general strategy to control the self-assembling properties of cyclodextrin platforms through the installation of a fluorescent probe that, at the same time, allows monitoring aggregation and inclusion properties. Further application of this concept in the design of functional derivatives for biomolecular complexation is currently sought in our laboratories.

ASSOCIATED CONTENT

S Supporting Information

Details of synthesis procedures, general reaction conditions, relevant spectroscopic data for compounds characterization and additional figures for the thermodynamics and molecular modeling analysis. This material is available free of charge via the Internet at <http://pubs.acs.org>.

AUTHOR INFORMATION

Notes

The authors declare no competing financial interest.

ACKNOWLEDGMENTS

This work was supported by the Universidad de Alcalá (GC2011-002 and UAH2011/EXP-036). The Spanish Ministerio de Economía y Competitividad (contract numbers CTQ2010-15848 and SAF2010-15670; cofinanced with the Fondo Europeo de Desarrollo Regional FEDER), the Junta de Andalucía, and the CSIC are also thanked. M.J.G.-A. acknowledges an FPU MICINN grant. F.M. and M.J.G.-A. acknowledge the assistance of M. L. Heijnen with the preparation of the manuscript.

REFERENCES

- (1) Dodziuk, H. *Cyclodextrins and Their Complexes*; Wiley-VCH Verlag GmbH & Co. KGaA: Weinheim, 2008; p 489.
- (2) Cyclodextrins. In *Macrocycles: Construction, Chemistry and Nanotechnology Applications*; Davis, F., Higson, S., Eds.; Wiley: Chichester, 2011; pp 190–254.
- (3) Easton, C. J.; Lincoln, S. F. *Modified Cyclodextrins, Scaffolds and Templates for Supramolecular Chemistry*; Imperial College Press: London, 2000.
- (4) Hattori, K.; Ikeda, H. Modifications reactions of cyclodextrins and the chemistry of modified cyclodextrins. In *Cyclodextrins and Their Complexes*; Dodziuk, H., Ed.; Wiley-VCH Verlag GmbH & Co. KGaA: Weinheim, 2008; pp 31–64.
- (5) Liu, Y.; Chen, Y. Cooperative Binding and Multiple Recognition by Bridged Bis(β-cyclodextrin)s with Functional Linkers. *Acc. Chem. Res.* **2006**, *39* (10), 681–691.
- (6) Chen, Y.; Zhang, Y.-M.; Liu, Y. Multidimensional Nanoarchitectures Based on Cyclodextrins. *Chem. Commun.* **2010**, *46* (31), 5622–5633.
- (7) Ogoshi, T.; Harada, A. Chemical Sensors Based on Cyclodextrin Derivatives. *Sensors* **2008**, *8* (8), 4961–4982.
- (8) Marchetti, L.; Levine, M. Biomimetic Catalysis. *ACS Catal.* **2011**, *1* (9), 1090–1118.
- (9) Zhao, W.; Zhong, Q. Recent Advance of Cyclodextrins as Nanoreactors in Various Organic Reactions: a Brief Overview. *J. Inclusion Phenom. Macrocyclic Chem.* **2012**, *72* (1–2), 1–14.
- (10) Ueno, A.; Kuwabara, T.; Nakamura, A.; Toda, F. A Modified Cyclodextrin as a Guest Responsive Color-Change Indicator. *Nature* **1992**, *356* (6365), 136–137.
- (11) Berberan-Santos, M. N.; Choppinet, P.; Fedorov, A.; Jullien, L.; Valeur, B. Multichromophoric Cyclodextrins. 8. Dynamics of Homomeric and Heterotransfer of Excitation Energy in Inclusion Complexes with Fluorescent Dyes. *J. Am. Chem. Soc.* **2000**, *122* (48), 11876–11886.
- (12) Freeman, R.; Finder, T.; Bahshi, L.; Willner, I. β-Cyclodextrin-Modified CdSe/ZnS Quantum Dots for Sensing and Chiroselective Analysis. *Nano Lett.* **2009**, *9* (5), 2073–2076.
- (13) Krishnaveni, R.; Ramamurthy, P.; Padma, M. E. J.; Divya, P. Synthesis and Characterization of NADH Model Compound Modified β-Cyclodextrin and Its Role as an Energy Donor in FRET. *J. Photochim. Photobiol. A* **2012**, *229* (1), 60–68.
- (14) Fang, G.; Xu, M.; Zeng, F.; Wu, S. β-Cyclodextrin as the Vehicle for Forming Ratiometric Mercury Ion Sensor Usable in Aqueous Media, Biological Fluids, and Live Cells. *Langmuir* **2010**, *26* (22), 17764–17771.
- (15) Berberan-Santos, M. N.; Cancéll, J.; Brochon, J. C.; Jullien, L.; Lehn, J. M.; Pouget, J.; Tauc, P.; Valeur, B. Multichromophoric Cyclodextrins. 1. Synthesis of O-naphthoyl-β-cyclodextrins and investigation of excimer formation and energy hopping. *J. Am. Chem. Soc.* **1992**, *114* (16), 6427–6436.
- (16) Toda, M.; Kondo, Y.; Hamada, F. Supramolecular Assembly System Depended on Guest Species Based on bis-Naphthalene Modified β-Cyclodextrin Dimer. *J. Inclusion Phenom. Macrocyclic Chem.* **2007**, *59* (3–4), 341–344.
- (17) Li, L.; Ke, C.-F.; Zhang, H.-Y.; Liu, Y. Coordination-Induced Switchable Nanoparticle Formation from Naphthyl-Bridged Bis(β-cyclodextrin). *J. Org. Chem.* **2010**, *75* (19), 6673–6676.
- (18) Fukuhara, G.; Mori, T.; Inoue, Y. Competitive Enantiodifferentiating Anti-Markovnikov Photoaddition of Water and Methanol to 1,1-Diphenylpropene Using A Sensitizing Cyclodextrin Host. *J. Org. Chem.* **2009**, *74* (17), 6714–6727.
- (19) Kikuchi, T.; Narita, M.; Hamada, F. Synthesis of bis Dansyl-Modified β-Cyclodextrin Liner Trimer Having Multi-Recognition Sites and High Hydrophobic Environment. *Tetrahedron* **2001**, *57* (45), 9317–9324.
- (20) Liu, Y.; Shi, J.; Guo, D.-S. Novel Permethylated β-Cyclodextrin Derivatives Appended with Chromophores as Efficient Fluorescent Sensors for the Molecular Recognition of Bile Salts. *J. Org. Chem.* **2007**, *72* (22), 8227–8234.
- (21) Nakashima, H.; Yoshida, N. Fluorescent Detection for Cyclic and Acyclic Alcohol Guests by Naphthalene-Appended Amino-β-Cyclodextrins. *Org. Lett.* **2006**, *8* (22), 4997–5000.
- (22) Díaz-Moscoso, A.; Vercauteren, D.; Rejman, J.; Benito, J. M.; Ortiz Mellet, C.; de Smedt, S. C.; García Fernández, J. M. Insights in Cellular Uptake Mechanisms of pDNA-Polycationic Amphiphilic Cyclodextrin Nanoparticles (CDplexes). *J. Controlled Release* **2010**, *143* (3), 318–325.
- (23) Díaz-Moscoso, A.; Guilloteau, N.; Bienvenu, C.; Méndez-Ardoy, A.; Jiménez Blanco, J. L.; Benito, J. M.; Le Gourriérec, L.; Di Giorgio, C.; Vierling, P.; Defaye, J.; et al. Mannosyl-Coated Nanocomplexes from Amphiphilic Cyclodextrins and pDNA for Site-Specific Gene Delivery. *Biomaterials* **2011**, *32* (29), 7263–7273.
- (24) Symens, N.; Méndez-Ardoy, A.; Díaz-Moscoso, A.; Sánchez-Fernández, E.; Remaut, K.; Demeester, J.; García Fernández, J. M.; de Smedt, S. C.; Rejman, J. Efficient Transfection of Hepatocytes Mediated by mRNA Complexed to Galactosylated Cyclodextrins. *Bioconjugate Chem.* **2012**, *23* (6), 1276–1289.
- (25) Ortiz Mellet, C.; Benito, J. M.; García Fernández, J. M. Preorganized, Macromolecular, Gene-Delivery Systems. *Chem.—Eur. J.* **2010**, *16*, 6728–6742.
- (26) Díaz-Moscoso, A.; Balbuena, P.; Gómez-García, M.; Ortiz Mellet, C.; Benito, J. M.; Le Gourriérec, L.; Di Giorgio, C.; Vierling, P.; Mazzaglia, A.; Micali, N.; et al. Rational Design of Cationic Cyclooligosaccharides as Efficient Gene Delivery Systems. *Chem. Commun.* **2008**, *7* (17), 2001–2003.
- (27) Díaz-Moscoso, A.; Le Gourriérec, L.; Gómez-García, M.; Benito, J. M.; Balbuena, P.; Ortega-Caballero, F.; Guilloteau, N.; Di Giorgio, C.; Vierling, P.; Defaye, J.; et al. Polycationic Amphiphilic Cyclodextrins for Gene Delivery: Synthesis and Effect of Structural Modifications on Plasmid DNA Complex Stability, Cytotoxicity, and Gene Expression. *Chem.—Eur. J.* **2009**, *15* (46), 12871–12888.
- (28) Méndez-Ardoy, A.; Gómez-García, M.; Ortiz Mellet, C.; Sevillano, N.; Girón, M. D.; Salto, R.; Santoyo-González, F.; García Fernández, J. M. Preorganized Macromolecular Gene Delivery Systems: Amphiphilic -Cyclodextrin Click Clusters. *Org. Biomol. Chem.* **2009**, *7*, 2681–2684.
- (29) Méndez-Ardoy, A.; Guilloteau, N.; Di Giorgio, C.; Vierling, P.; Santoyo-González, F.; Ortiz Mellet, C.; García Fernández, J. M. β-Cyclodextrin-Based Polycationic Amphiphilic “Click” Clusters: Effect of Structural Modifications in Their DNA Complexing and Delivery Properties. *J. Org. Chem.* **2011**, *76* (15), 5882–5894.
- (30) Bienvenu, C.; Martínez, A.; Jiménez Blanco, J. L.; Di Giorgio, C.; Vierling, P.; Ortiz Mellet, C.; Defaye, J.; García Fernández, J. M. Polycationic Amphiphilic Cyclodextrins as Gene Vectors: Effect of the Macroyclic Ring Size on the DNA Complexing and Delivery Properties. *Org. Biomol. Chem.* **2012**, *10* (29), 5570–5581.
- (31) Rekharsky, M. V.; Inoue, Y. Complexation Thermodynamics of Cyclodextrins. *Chem. Rev.* **1998**, *98* (5), 1875–1917.
- (32) Sau, S.; Solanki, B.; Orpicio, R.; Van, S. J.; Evans, C. H. Higher-Order Cyclodextrin Complexes: The Naphthalene System. *J. Inclusion Phenom. Macrocyclic Chem.* **2004**, *48* (3–4), 173–180.

- (33) Harada, A.; Hashidzume, A.; Yamaguchi, H.; Takashima, Y. CD-Based Polymeric Rotaxanes. *Chem. Rev.* **2009**, *109* (11), 5974–6023.
- (34) Li, J.; Ni, X.; Zhou, Z.; Leong, K. W. Preparation and Characterization of Polypseudorotaxanes Based on Block-Selected Inclusion Complexation between Poly(propylene oxide)-Poly(ethylene oxide)-Poly(propylene oxide) Triblock Copolymers and α -Cyclodextrin. *J. Am. Chem. Soc.* **2003**, *125* (7), 1788–1795.
- (35) Xu, H.-X.; Cheng, S.-F.; Yang, X.-J.; Chen, B.; Chen, Y.; Zhang, L.-P.; Wu, L.-Z.; Fang, W.; Tung, C.-H.; Weiss, R. G. Enhancement of Diastereoselectivity in Photodimerization of Alkyl 2-Naphthoates with Chiral Auxiliaries via Inclusion within γ -Cyclodextrin Cavities. *J. Org. Chem.* **2012**, *77* (4), 1685–1692.
- (36) Nakamura, A.; Inoue, Y. Electrostatic Manipulation of Enantio-Differentiating Photo-Cyclodimerization of 2-Anthracenecarboxylate within γ -Cyclodextrin Cavity through Chemical Modification. Inverted Product Distribution and Enhanced Enantioselectivity. *J. Am. Chem. Soc.* **2005**, *127* (15), 5338–5339.
- (37) Yang, C.; Mori, T.; Origane, Y.; Ko, Y. H.; Selvapalam, N.; Kim, K.; Inoue, Y. Highly Stereoselective Photocyclodimerization of α -Cyclodextrin-Appended Anthracene Mediated by γ -Cyclodextrin and Cucurbit[8]uril: A Dramatic Steric Effect Operating Outside the Binding Site. *J. Am. Chem. Soc.* **2008**, *130* (27), 8574–8575.
- (38) Wang, Q.; Yang, C.; Ke, C.; Fukuhara, G.; Mori, T.; Liu, Y.; Inoue, Y. Wavelength-Controlled Supramolecular Photocyclodimerization of Anthracenecarboxylate Mediated by γ -Cyclodextrins. *Chem. Commun.* **2011**, *47* (24), 6849–6851.
- (39) Yang, C.; Ke, C.; Liang, W.; Fukuhara, G.; Mori, T.; Liu, Y.; Inoue, Y. Dual Supramolecular Photochirogenesis: Ultimate Stereo-control of Photocyclodimerization by a Chiral Scaffold and Confining Host. *J. Am. Chem. Soc.* **2011**, *133* (35), 13786–13789.
- (40) Ke, C.; Yang, C.; Mori, T.; Wada, T.; Liu, Y.; Inoue, Y. Catalytic Enantiodifferentiating Photocyclodimerization of 2-Anthracenecarboxylic Acid Mediated by a Non-Sensitizing Chiral Metallosupramolecular Host. *Angew. Chem., Int. Ed.* **2009**, *48* (36), 6675–6677.
- (41) Ueno, A.; Tomita, Y.; Osa, T. Excimer Formation in the Cavity of γ -Cyclodextrin Appended by a Naphthalene Moiety. *Chem. Lett.* **1983**, No. 10, 1635–1638.
- (42) Ueno, A.; Moriwaki, F.; Osa, T.; Hamada, F.; Murai, K. Exciton Coupling, Excimer Emission and Unique Binding Behavior of γ -Cyclodextrin Substituted by Two Naphthyl Residues. *Tetrahedron Lett.* **1985**, *26* (28), 3339–3342.
- (43) Moriwaki, F.; Kaneko, H.; Ueno, A.; Osa, T.; Hamada, F.; Murai, K. Excimer Formation and Induced-Fit Type of Complexation of b-Cyclodextrin Capped by Two Naphthyl Moieties. *Bull. Chem. Soc. Jpn.* **1987**, *60* (10), 3619–3623.
- (44) Ueno, A.; Moriwaki, F.; Osa, T.; Hamada, F.; Murai, K. Excimer Formation in Inclusion Complexes of Modified Cyclodextrins. *Tetrahedron* **1987**, *43* (7), 1571–1578.
- (45) Ueno, A.; Tomita, Y.; Osa, T. Association of Naphthalene-Appended γ -Cyclodextrin with β -Cyclodextrin. *J. Chem. Soc., Chem. Commun.* **1983**, *24*, 1515–1516.
- (46) Ueno, A.; Tomita, Y.; Osa, T. Promoted Binding Ability of γ -Cyclodextrin Appended by a Space-Regulating Naphthalene Moiety. *J. Chem. Soc., Chem. Commun.* **1983**, *17*, 976–977.
- (47) Ueno, A.; Moriwaki, F.; Tomita, Y.; Osa, T. Fluorescence Quenching in Host-Guest Complexes of Modified γ -Cyclodextrin. *Chem. Lett.* **1985**, *4*, 493–496.
- (48) Ueno, A.; Moriwaki, F.; Osa, T.; Hamada, F.; Murai, K. Fluorescence and Circular Dichroism Studies on Host-Guest Complexation of g-Cyclodextrin Bearing Two 2-Naphthyl Moieties. *Bull. Chem. Soc. Jpn.* **1986**, *59* (2), 465–470.
- (49) Hamada, F.; Minato, S.; Osa, T.; Ueno, A. Fluorescent Sensors for Molecules. Guest-Responsive Monomer and Excimer Fluorescence of 6A,6B-; 6A,6C-; 6A,6D-; and 6A,6E-bis(2-Naphthylsulfonyl)- γ -cyclodextrins. *Bull. Chem. Soc. Jpn.* **1997**, *70* (6), 1339–1346.
- (50) Minato, S.; Osa, T.; Ueno, A. Detection of Neutral Organic Compounds by Excimer-Forming Bichromophoric γ -Cyclodextrins. *J. Chem. Soc., Chem. Commun.* **1991**, *2*, 107–108.
- (51) Ueno, A.; Minato, S.; Osa, T. Host-Guest Sensors of 6A,6B-, 6A,6C-, 6A,6D-, and 6A,6E-bis(2-Naphthylsulfonyl)- γ -cyclodextrins for Detecting Organic Compounds by Fluorescence Enhancements. *Anal. Chem.* **1992**, *64* (10), 1154–1157.
- (52) Minato, S.; Osa, T.; Morita, M.; Nakamura, A.; Ikeda, H.; Toda, F.; Ueno, A. Intramolecular Excimer Formation and Molecular Recognition of Modified Cyclodextrins Appended by Two Naphthalene Rings. *Photochem. Photobiol.* **1991**, *54* (4), 593–597.
- (53) Moriwaki, F.; Kaneko, H.; Ueno, A.; Osa, T.; Hamada, F.; Murai, K. Excimer Formation and Induced-Fit Type of Complexation of β -Cyclodextrin Capped by Two Naphthyl Moieties. *Bull. Chem. Soc. Jpn.* **1987**, *60* (10), 3619–3623.
- (54) Tamura, M.; Gao, D.; Ueno, A. A Polyrotaxane Series Containing α -Cyclodextrin and Naphthalene-Modified α -Cyclodextrin as a Light-Harvesting Antenna System. *Chem.—Eur. J.* **2001**, *7* (7), 1390–1397.
- (55) Tamura, M.; Ueno, A. Energy Transfer in a Rotaxane with a Naphthalene-Modified α -Cyclodextrin Threaded by Dansyl-Terminal Poly(ethylene glycol). *Chem. Lett.* **1998**, *4*, 369–370.
- (56) Tamura, M.; Ueno, A. Energy Transfer and Guest Responsive Fluorescence Spectra of Polyrotaxane Consisting of α -Cyclodextrins Bearing Naphthyl Moieties. *Bull. Chem. Soc. Jpn.* **2000**, *73* (1), 147–154.
- (57) Tamura, M.; Guo, D.; Ueno, A. A Series of Polyrotaxanes Containing α -Cyclodextrin and Naphthalene-Modified α -Cyclodextrin and Solvent Effects on the Fluorescence Quenching by Terminal Units. *J. Chem. Soc., Perkin Trans. 2* **2001**, No. 10, 2012–2021.
- (58) Joung, Y.-K.; Choi, H. S.; Ooya, T.; Yui, N. 1H NMR Titration Study of Stimuli-Responsive Supramolecular Assemblies: Inclusion Complexes between PEG-b-PEI Copolymer-Grafted Dextran and Naphthalene-Appended γ -Cyclodextrin via Double-Strand Inclusion. *J. Inclusion Phenom. Macrocyclic Chem.* **2007**, *57* (1–4), 323–328.
- (59) Park, J. W.; Lee, S. Y.; Kim, S. M. Efficient Inclusion Complexation and Intra-Complex Excitation Energy Transfer between Aromatic Group-Modified β -Cyclodextrins and a Hemicyanine Dye. *J. Photochem. Photobiol., A* **2005**, *173* (3), 271–278.
- (60) Park, J. W.; Song, H. E.; Lee, S. Y. Face Selectivity of Inclusion Complexation of Viologens with β -Cyclodextrin and 6-O-(2-Sulfonato-6-naphthyl)- β -cyclodextrin. *J. Phys. Chem. B* **2002**, *106* (29), 7186–7192.
- (61) Park, J. W.; Song, H. E.; Lee, S. Y. Facile Dimerization and Circular Dichroism Characteristics of 6-O-(2-Sulfonato-6-naphthyl)-b-cyclodextrin. *J. Phys. Chem. B* **2002**, *106* (20), 5177–5183.
- (62) Park, J. W.; Song, H. E.; Lee, S. Y. Homo-Dimerization and Hetero-Association of 6-O-(2-Sulfonato-6-naphthyl)-g-cyclodextrin and 6-Deoxy-(pyrene-1-carboxamido)-b-cyclodextrin. *J. Org. Chem.* **2003**, *68* (18), 7071–7076.
- (63) Park, J. W.; Lee, S. Y.; Kim, S. M. Efficient Inclusion Complexation and Intra-Complex Excitation Energy Transfer between Aromatic Group-Modified b-Cyclodextrins and a Hemicyanine Dye. *J. Photochem. Photobiol., A* **2005**, *173* (3), 271–278.
- (64) Park, J. W.; Lee, S. Y.; Song, H. J.; Park, K. K. Self-Inclusion Behavior and Circular Dichroism of Aliphatic Chain-Linked b-Cyclodextrin-Viologen Compounds and Their Reduced Forms Depending on the Side of Modification. *J. Org. Chem.* **2005**, *70* (23), 9505–9513.
- (65) Gamieldien, M. R.; Maestre, I.; Jaime, C.; Naidoo, K. J. Optimal Configurations of “Capped” b-Cyclodextrin Dimers in Water Maximise Hydrophobic Association. *ChemPhysChem* **2010**, *11* (2), 452–459.
- (66) González-Álvarez, M. J.; Méndez-Ardoy, A.; Benito, J. M.; García Fernández, J. M.; Mendicuti, F. Self-Association of a Naphthalene-Capped- β -Cyclodextrin through Cooperative Strong Hydrophobic Interactions. *J. Photochem. Photobiol., A* **2011**, *223* (1), 25–36.
- (67) Mellet, C. O.; Fernandez, J. M. G.; Benito, J. M. Cyclodextrin-Based Gene Delivery Systems. *Chem. Soc. Rev.* **2011**, *40* (3), 1586–1608.

- (68) Balbuena, P.; Lesur, D.; González-Álvarez, M. J.; Mendicuti, F.; Ortiz Mellet, C.; García Fernández, J. M. One-Pot Regioselective Synthesis of 2I,3I-O-(*o*-Xylylene)-Capped Cyclomalto-Oligosaccharides: Tailoring the Topology and Supramolecular Properties of Cyclodextrins. *Chem. Commun.* **2007**, *31*, 3270–3272.
- (69) González-Álvarez, M. J.; Balbuena, P.; Ortiz Mellet, C.; García Fernández, J. M.; Mendicuti, F. Study of the Conformational and Self-Aggregation Properties of 2I,3I-O-(*o*-Xylylene)-per-O-Me-*a*- and -*b*-Cyclodextrins by Fluorescence and Molecular Modeling. *J. Phys. Chem. B* **2008**, *112* (44), 13717–13729.
- (70) González-Álvarez, M. J.; Vicente, J.; Ortiz Mellet, C.; García Fernández, J. M.; Mendicuti, F. Thermodynamics of the Dimer Formation of 2I,3I-O-(*o*-Xylylene)-per-O-Me-*g*-cyclodextrin: Fluorescence, Molecular Mechanics and Molecular Dynamics. *J. Fluoresc.* **2009**, *19* (6), 975–988.
- (71) O'Connor, D. V.; Ware, W. R.; Andre, J. C. Deconvolution of Fluorescence Decay Curves. A Critical Comparison of Techniques. *J. Phys. Chem.* **1979**, *83* (10), 1333–1343.
- (72) Lakowicz, J. R. Quenching of Fluorescence. In *Principles of Fluorescence Spectroscopy*, 3rd ed.; Lakowicz, J. R., Ed.; Springer: New York, 2008; p 280.
- (73) Sybyl-X 1.2, Tripos International, 1699 South Hanley Rd., St. Louis, Missouri, 63144, USA.
- (74) Clark, M.; Cramer, R. D., III; Van, O. N. Validation of the General Purpose Tripos 5.2 Force Field. *J. Comput. Chem.* **1989**, *10* (8), 982–1012.
- (75) Frisch, M. J.; et al. MOPAC (AM1), included in the Gaussian 03 package, *Gaussian 03*, revision C.02; Gaussian, Inc.: Wallingford, CT, 2004.
- (76) Brunel, Y.; Faucher, H.; Gagnaire, D.; Rassat, A. Program of Minimization of the Empirical Energy of a Molecule by a Simple Method. *Tetrahedron* **1975**, *31* (8), 1075–1091.
- (77) Press, W. H.; Teukolsky, S. A.; Vetterling, W. T.; Flannery, B. P. *Numerical Recipes: The Art of Scientific Computing*, 3rd ed.; Cambridge University Press: Cambridge, U.K., 2007.
- (78) Blanco, M. Molecular Silverware. I. General Solutions to Excluded Volume Constrained Problems. *J. Comput. Chem.* **1991**, *12* (2), 237–247.
- (79) González-Álvarez, M. J.; Di Marino, A.; Mendicuti, F. Fluorescence, Induced Circular Dichroism and Molecular Mechanics of 1-Methyl Naphthalenecarboxylate Complexes with 2-Hydroxypropyl Cyclodextrins. *J. Fluoresc.* **2009**, *19* (3), 449–462.
- (80) Harata, K.; Ueda, H. Circular Dichroism Spectra of the *b*-Cyclodextrin Complex with Naphthalene Derivatives. *Bull. Chem. Soc. Jpn.* **1975**, *48* (2), 375–378.
- (81) Platt, J. R. Classification of Spectra of cata-Condensed Hydrocarbons. *J. Chem. Phys.* **1949**, *17*, 484–495.
- (82) Kodaka, M. Application of a General Rule to Induced Circular Dichroism of Naphthalene Derivatives Complexed with Cyclodextrins. *J. Phys. Chem. A* **1998**, *102* (42), 8101–8103.
- (83) Park, J. W.; Song, H. E.; Lee, S. Y. Homo-Dimerization and Hetero-Association of 6-O-(2-Sulfonato-6-naphthyl)- γ -cyclodextrin and 6-Deoxy-(pyrene-1-carboxamido)- β -cyclodextrin. *J. Org. Chem.* **2003**, *68* (18), 7071–7076.
- (84) Park, J. W.; Song, H. E.; Lee, S. Y. Facile Dimerization and Circular Dichroism Characteristics of 6-O-(2-Sulfonato-6-naphthyl)- β -cyclodextrin. *J. Phys. Chem. B* **2002**, *106* (20), 5177–5183.
- (85) McAlpine, S. R.; Garcia-Garibay, M. A. Studies of Naphthyl-Substituted *b*-Cyclodextrins. Self-Aggregation and Inclusion of External Guests. *J. Am. Chem. Soc.* **1998**, *120* (18), 4269–4275.
- (86) Mendicuti, F. Applications of Fluorescence Techniques and Modeling to the Study of the Complexation of Chromophore-Containing Guests with Cyclodextrins. *Trends Phys. Chem.* **2006**, *11*, 61–77.
- (87) Usero, R.; Alvariza, C.; González-Álvarez, M. J.; Mendicuti, F. Complexation of Dimethyl 2,3-Naphthalenedicarboxylate with 2-Hydroxypropyl- α , β - and γ -Cyclodextrins in Aqueous Solution by Fluorescence, Circular Dichroism and Molecular Mechanics. *J. Fluoresc.* **2008**, *18* (6), 1103–1114.
- (88) Alvariza, C.; Usero, R.; Mendicuti, F. Binding of Dimethyl 2,3-Naphthalenedicarboxylate with α -, β - and γ -Cyclodextrins in Aqueous Solution. *Spectrochim. Acta, Part A* **2007**, *67* (2), 420–429.
- (89) Cromwell, W. C.; Bystrom, K.; Eftink, M. R. Cyclodextrin-Adamantanecarboxylate Inclusion Complexes: Studies of the Variation in Cavity Size. *J. Phys. Chem.* **1985**, *89* (2), 326–332.
- (90) Lo, M. P.; D'Anna, F.; Riela, S.; Gruttaduria, M.; Noto, R. Host-Guest Interactions Involving Cyclodextrins: Useful Complementary Insights Achieved by Polarimetry. *Tetrahedron* **2007**, *63* (37), 9163–9171.
- (91) Eftink, M. R.; Andy, M. L.; Bystrom, K.; Perlmutter, H. D.; Kristol, D. S. Cyclodextrin Inclusion Complexes: Studies of the Variation in the Size of Alicyclic Guests. *J. Am. Chem. Soc.* **1989**, *111* (17), 6765–6772.
- (92) Kodaka, M. Sign of Circular Dichroism Induced by *b*-Cyclodextrin. *J. Phys. Chem.* **1991**, *95* (6), 2110–2112.
- (93) Kodaka, M. A General Rule for Circular Dichroism Induced by a Chiral Macrocycle. *J. Am. Chem. Soc.* **1993**, *115* (9), 3702–3705.
- (94) Berova, N.; Nakanishi, K. Exciton Chirality Method: Principles and Applications. In *Circular Dichroism: Principles and Applications*; Berova, N., Nakanishi, K., Woody, R. W., Eds.; Wiley-VCH: New York, 2000; pp 337–382.